J Solid State Electrochem
DOI 10.1007/s10008-011-1429-1

ORIGINAL PAPER

Irreversible electrostatic deposition of Prussian blue from colloidal solutions

Regina Cisternas · Eduardo Muñoz · Rodrigo Henríquez · Ricardo Córdova · Heike Kahlert · Ulrich Hasse · Fritz Scholz

Received: 4 March 2011 / Revised: 29 April 2011 / Accepted: 2 May 2011

Abstract Prussian blue (PB) can be deposited from colloidal solutions (5.4×10^{-3} $mol_{PB}L^{-1}$, 0.01 mol L^{-1} KNO_3) on glassy carbon, either by potential cycling or potentiostatically, provided that the deposition potential is more positive than −0.2 V vs. Hg/Hg_2Cl_2. Depending on the deposition potential, the PB particles form either a single layer of Everitt's salt, of PB, or multilayers of Berlin green. Also depending on the electrode potential, the deposition was accompanied by currents which were either only of capacitive nature, or represent the sum of capacitive and faradaic currents. The currents were always limited by the diffusion of the colloidal particles to the electrode surface, i.e., they obeyed the Cottrell equation. The PB layers were characterized by in situ atomic force microscopy.

Keywords Particle deposition · Prussian blue · Atomic force microscopy

The authors dedicate this contribution to Professor Dr. George Inzelt on the occasion of his 65th birthday.

R. Cisternas · E. Muñoz · R. Henríquez · R. Córdova
Pontificia Universidad Católica de Valparaíso,
Facultad de Ciencias,
Avda. Universidad 330,
Valparaíso, Chile

H. Kahlert · U. Hasse · F. Scholz (✉)
Institut für Biochemie, Universität Greifswald,
Felix-Hausdorff-Straße 4,
17487 Greifswald, Germany
e-mail: fscholz@uni-greifswald.de

Introduction

Prussian blue (PB) is a frequently exploited surface modifier of electrodes because it possesses electrocatalytic properties and can be used for mediating the electron transfer to various redox systems [1, 2, 3]. The electrochemistry of PB has been extensively studied and is very well-documented [4, 5, 6]. The first method to deposit PB on an electrode has been based on a spontaneous deposition of PB on a Pt electrode in a solution containing Fe(III) ions and ferrocyanide [7], and later electrochemical procedures have been developed [8, 9]. These methods allow depositing stable films; however, the composition of the film cannot be easily controlled. A method which allows depositing well-characterized PB is the mechanical immobilization of solid PB on the surface of an electrode [10, 11]. Additionally, a plethora of other methods exists for deposition of PB and its composites on electrodes (e.g., [12, 13]).

Colloidal particles can acquire a surface charge by (1) adsorption of ions according to the Paneth-Fajans rule [14, 15, 16], or (2) by a surface dissociation processes [17]. Decreasing ionic strength leads to an increasing Debye length of the double layer enveloping the particles and thus stabilizes the colloids according to the DLVO theory [18]. Colloidal particles can be deposited on charged surfaces, e.g., electrodes, provided that the electrostatic interactions are favorable, or strong adsorption helps to overcome electrostatic repulsion. The deposition can be irreversible if—once the particles are attached—strong van der Waals forces keep the particles immobile on the surface. Colloidal PB particles dispersed in aqueous solution are known to have a negative surface charge

Published online: 13 May 2011

[19]. This also accounts for the adherence of colloidal PB particles to the surface of negatively charged goethite [19], and it is used to deposit PB layers on charged surfaces by so-called electrostatic self-assembly [20]. Hence, it was supposed that they will attach also to a positively charged electrode surface. Indeed, it has been observed previously that a cyclic polarization of a glassy carbon electrode shows a slowly increasing electrochemical pattern of PB [21]. Here, we report this as a new method based on the irreversible electrostatic deposition of PB from colloidal solutions. It should be mentioned that the electrostatic deposition of colloidal particles is the basis of the so-called electrophoretic painting [22] utilized on a large industrial scale.

Experimental section

PB has been synthesized as follows: 250 mL of a solution containing 5×10^{-2} mol L^{-1} Fe(III) (prepared with $FeCl_3\times6H_2O$) and 0.01 mol L^{-1} KCl were thoroughly stirred, and 250 mL of a solution containing 5.2×10^{-2} mol L^{-1} of $K_4[Fe(CN)_6]\times3H_2O$ were drop-wise added. The mixture was kept at 40°C for 2 h. Once the solution has reached room temperature, it was centrifuged with the aim of separating the precipitate, which was washed two times with double-distilled water. The washed precipitate was dried in a stove at 60°C. Later, the solid was mixed with a small quantity of water to form a paste which was stored in a flask. Colloidal PB solutions were prepared by dissolving 0.05 g of the paste and 0.25 g of KNO_3 in 250 mL of water. The electrolytic solutions were prepared using distilled and deionized water (Millipore) with a resistivity of 18 MΩ cm. Analytical grade reagents from Merck ($FeCl_3\times6H_2O$, $K_4[Fe(CN)_6]\times3H_2O$, KCl, KNO_3) were used. A glassy carbon electrode (r= 0.125 mm; surface area 0.049 cm^2) was used as working electrode which was mechanically cleaned before each measurement using the following procedure: polishing for 5 min using a cloth impregnated with 5-μm alumina, then polishing for 5 min with 0.3-μm alumina, and finally polishing for 5 min with 0.05-μm alumina. Eventually, the electrode was washed with deionized water in an ultrasonic bath for 10 min. A pure nitrogen stream was passed through the solution for 30 min before measurements, and over the solution during the experiments. A standard calomel electrode (Hg/Hg_2Cl_2, KCl-saturated; 0.244 V vs. SHE at 25°C) was used as reference electrode in all electrochemical experiments and all the potentials reported in this study refer to this reference electrode. All electrochemical measurements have been performed using an Ecochemie potentiostat/galvanostat equipment model Autolab PGSTAT20 interfaced to a PC. The atomic force micrographs have been recorded in situ with a Digital Instruments equipment model Nanoscope I with software SPM 43.2 v in contact mode and using as an electrochemical interface, an Autolab PGSTA20 equipment. The amount of deposited PB was determined by chronocoulometry as follows: first, the deposit (be it Prussian blue or Berlin green) was completely reduced to Everitt's salt (Fe^{2+}_{hs}), and then the charge of oxidation of Everitt's salt to PB (Fe^{3+}_{hs}) was measured. To calculate the amount of PB, it has been assumed that 1 mol PB contains 1 mol high-spin iron, which is—especially in view of the preparation of the PB—a very good approximation.

Results

Electrochemical behavior of colloidal Prussian blue solutions at the glassy carbon electrode

Figure 1 shows the first and 25th cycles of successive cyclic voltammograms recorded in a quiet colloidal PB solution using a GC electrode (electrolyte, 0.01 mol L^{-1} KNO_3). The voltammograms were started at the open circuit potential (OCP=0.2 V), the potential scan was reversed at −0.3 V, and then extended to 1.2 V, with the following cycles between −0.3 and 1.2 V.

The typical PB response builds up, although slowly and not well-defined. Therefore, the deposition by potentiodynamic cycling was repeated for another three times, with 25 cycles each time. After these four series of 25 cycles, the electrode was washed and transferred to a solution containing 0.5 mol L^{-1} KNO_3. The OCP of the electrode was now 0.63 V. The cyclic voltammogram was started and recorded between −0.37 and 1.2 V (Fig. 2). Now, after these 100 potentiodynamic depositions cycles, reasonably well-developed signals typical for PB were observed: the system at the mid-peak potential E_{mp}=0.21 V is due to the

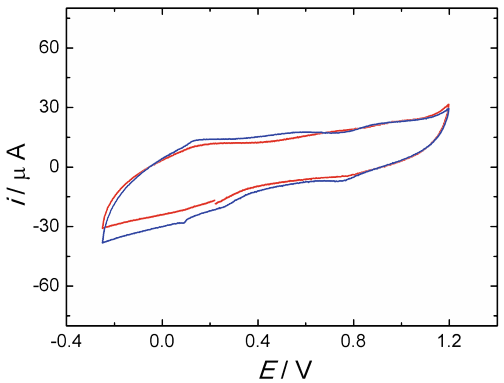

Fig. 1 Cyclic voltammograms recorded during the potentiodynamic deposition of Prussian blue on glassy carbon. *Red line* first cycle, *blue line* 25th cycle. Scan rate 0.1 Vs^{-1}, 5.4×10^{-3} $mol_{PB}L^{-1}$, 0.01 mol L^{-1} KNO_3

high-spin iron, and the system at the mid-peak potential E_{mp}=0.84 V is due to the low-spin iron of PB. Similar responses were observed for PB on other substrates [23, 24, 25, 26, 27, 28, 29, 30, 31]. The electrochemistry of PB can be summarized as follows:

$$\{K_2Fe^{2+}_{hs}[Fe^{2+}_{ls}(CN)_6]\}_{solid} \underset{+K^+ + e^-}{\overset{-K^+ - e^-}{\rightleftharpoons}} \{KFe^{3+}_{hs}[Fe^{2+}_{ls}(CN)_6]\}_{solid} \underset{+K^+ + e^-}{\overset{-K^+ - e^-}{\rightleftharpoons}} \{Fe^{3+}_{hs}[Fe^{3+}_{ls}(CN)_6]\}_{solid}$$

Everitt′ssalt — Prussian blue — Berlin green

From the results shown in Figs. 1 and 2, it is clear that PB is deposited during the potentiodynamic cycling; however, it is not clear at which potentials the PB is deposited. Furthermore, these results prove that the potentiodynamic deposition from unstirred solutions is a rather slow process; most probably because the colloidal PB particles have small diffusion coefficients. Therefore, experiments were performed in which PB was deposited at constant potentials and from stirred solutions. Stirring was accomplished in the standard electrochemical cell of the Metrohm electrode stands with the stirrer setting "3". Such experiments should give information on the potential dependence of deposition, and they should be also much more efficient with respect to the deposition rate. Figure 3 shows the chronoamperograms recorded during PB deposition at three different potentials in stirred solutions. These curves clearly show that PB undergoes a reduction reaction at 0 V (negative current), and an oxidation reaction at 0.8 V (positive current). The reduction current at 0 V deposition clearly indicates that the deposit is reduced to Everitt's salt (Fe^{2+}_{hs}). Interestingly, a positive current is observed at 0.5 V: this cannot be a faradaic current because PB (high-spin Fe (III) and low-spin Fe(II)) is not undergoing any faradaic reaction at that potential. Hence, the positive current must be the result of the interaction of the negatively charged PB particles with the positively charged glassy carbon electrode: when the approaching negatively charged PB particles have a higher surface charge density than the positively charged electrode, the latter must be further charged upon attachment, and this will cause a positive current.

To analyze the nature of the currents shown in Fig. 3, experiments were performed in an unstirred solution, and the currents were plotted versus the square root of time: Figure 4 shows that the system exhibits Cottrell behavior, i.e., the currents are diffusion controlled in unstirred solutions. The different slopes at the two different potential can be easily explained with a different number of involved electrons: As explained before, at 0.8 V a faradaic oxidation of the low-spin Fe(II) occurs, and additionally, electrons will flow due to the formation of a new interface (GC|$PB_{deposited}$) and a new interface $PB_{deposited}$|solution.

Considering the processes occurring at the interface, the current flow must consist of two contributions: (1) Attachment of the charged colloidal particles will alter the electric double layer structure of the electrode (formation of $PB_{deposited}$| solution), and also form another interface (GC|$PB_{deposited}$). (2) Depending on the electrode potential, the attached colloidal PB particles can be either reduced, remain unchanged, or being oxidized, i.e., they can produce a faradaic current. Both contributions need the particles to diffuse from the bulk solution to the electrode surface, so that the sum of both contributions will be diffusion-controlled,

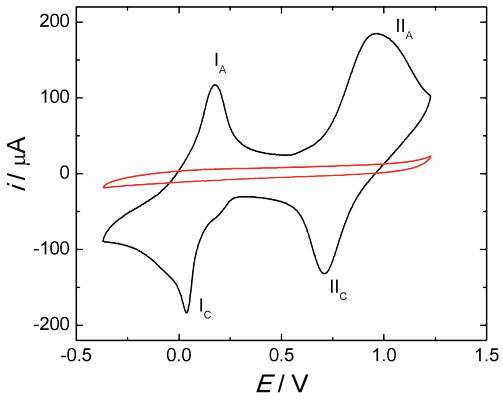

Fig. 2 Cyclic voltammogram of the GC/PB modified electrode (*black line*) and of bare GC (*red line*) in an electrolyte containing 0.5 mol L^{-1} KNO_3. Scan rate 0.1 Vs^{-1}

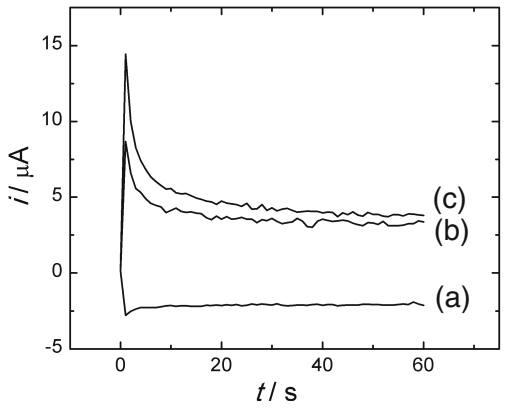

Fig. 3 Current transients for the PB thin film formation from colloidal solution onto glassy carbon in stirred solution. E_{dep} **a** 0.0 V, **b** 0.5 V, and (**c**) 0.8 V

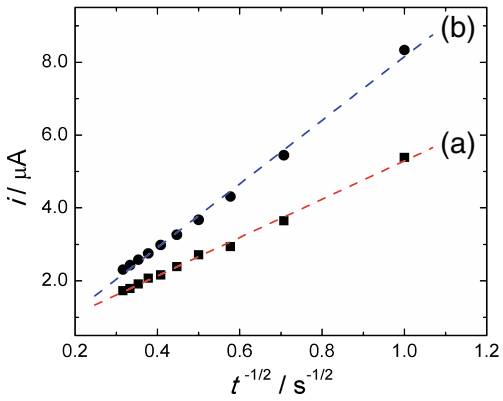

Fig. 4 Cottrell plot corresponding to the PB formation on GC under unstirred solution. E_{dep}: **a** 0.5 V and **b** 0.8 V

provided that the faradaic current due to the insertion electrochemistry of PB is not kinetically slowed down. It is well known for PB layers that the latter is not the case.

Now, we present the dependence of the amount of deposited PB on potential: For this to be determined, the electrode was washed with water following the PB deposition, transferred to a KNO_3 solution (0.5 mol L^{-1}), preconditioned for 60 s at −0.37 V in order to completely convert the PB to Everitt's salt (reduced form), and then the charge for oxidation to PB was measured with the help of chronocoulometry at 0.5 V within 1,000 s. These results are shown in Fig. 5.

Figure 5a shows that below a deposition potential of −0.2 V, there is no PB deposition on the electrode. At potentials higher than −0.2 V, PB is deposited and the potential dependence is wave-shaped. In the range from about 0 to 0.75 V, the deposition rate has a rather constant value, and at potentials exceeding 0.75 V, there is a second increase in deposition rate. In order to obtain reliable data for the higher deposition rate at potentials above 0.75 V, these measurements have been repeated with a shorter deposition time (60 s), and Fig. 5b shows the results. Obviously, there is a rather constantly ascending deposition rate above 0.75 V. Unfortunately, the measurements cannot be extended to potentials larger than 1.2 V for reasons of oxygen evolution.

The wave shape of the potential dependence of deposition rate (Fig. 5a) poses the question of the time-dependence of deposited PB. Figure 6 (black open circles) shows the amount of PB deposited at 0.5 V in the deposition-time range from 60 to 3,600 s. Clearly, the amount of deposited PB remains constant. This indicates that a certain layer of PB is deposited which cannot grow with time. This perfectly explains also the wave shape of the potential dependence. However, to understand the reason for the formation of a "single layer" (or monolayer), one needs to assume that in the potential range of the upper part of the wave, the PB particles attach to the glassy carbon maintaining their surface charge. This surface charge will not allow that charged PB particles from the solution can attach to them. The explanation can be found in a paper of Neff [32], who has shown that the conductivity of PB is very small (insulator) as $KFe^{3+}_{hs}[Fe^{2+}_{ls}(CN)_6]$, i.e., the Prussian blue state, and much larger (semiconductor) when the compound is oxidized to $Fe^{3+}_{hs}[Fe^{3+}_{ls}(CN)_6]$, i.e., in the Berlin green state. This means that in the potential range where $KFe^{3+}_{hs}[Fe^{2+}_{ls}(CN)_6]$ is stable, the particles behave as an insulator. At potentials above 0.8 V, the PB is converted to Berlin green, and the particles can be charged to the electrode potential which supports the further attachment of PB particles from the colloidal solution. In complete accordance with this, Fig. 6 (red circles) shows that the amount of PB attached to the glassy carbon electrode at 1.2 V is increasing with time, i.e.,

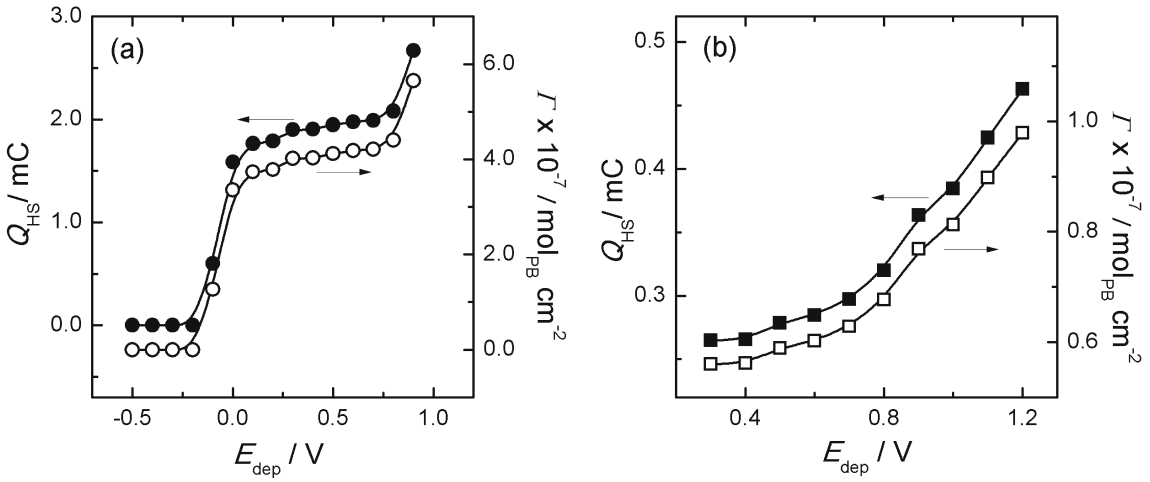

Fig. 5 Oxidation charge for high-spin iron (Q_{HS}) and amount of PB per surface area (Γ) as function of the PB deposition potential (E_{dep}). The time associated with E_{dep} of PB from the colloidal solution was: **a** 180 s, **b** 60 s. The amount of PB (in moles) was determined by chronocoulometry, as outlined in the experimental part

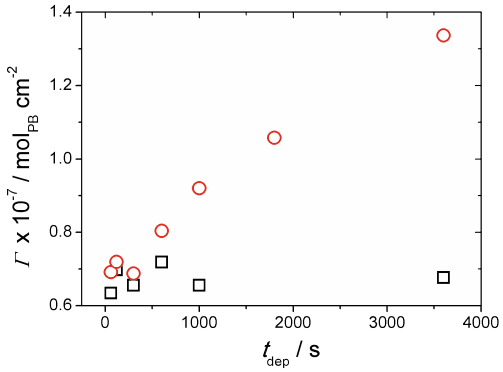

Fig. 6 Dependence of the amount of PB deposited at 0.5 V (*black squares*) and 1.2 V (*red circles*) as a function of deposition time. The amount of PB (in moles) was determined by chronocoulometry, as outlined in the Experimental section

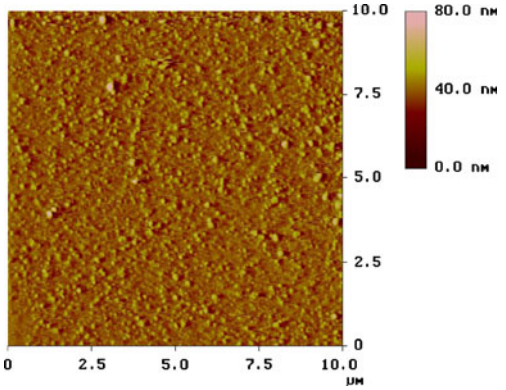

Fig. 8 In situ AFM images of a silicon sample with PB deposited from the colloidal solution at E_{dep}=0.45 V for 540 s

multilayers of deposited PB particles are formed when the deposit is in the Berlin green state. It is very important to note that the deposition of PB starts at potentials larger than −0.2 V vs. Hg/Hg_2Cl_2. The point of zero charge (PZC) of glassy carbon is in aqueous solution at pH 7 close to 0.0 V vs. Ag/AgCl that is close to −0.047 V vs. Hg/Hg_2Cl_2 [33]. From ac measurements with our glassy carbon electrodes, we could deduce a pzc of +0.053 V vs. Hg/Hg_2Cl_2. It is reasonable to assume that the pzc is also in the colloidal solutions around 0 V. This means that the deposition of PB (in the form of Everitt's salt) starts already at negative potentials with respect to the pzc, indicating a negative adsorption free energy which is caused by van der Waals forces between the deposit and glassy carbon.

Morphological analysis of PB particles deposited on GC electrode by means of in situ AFM

The morphology of deposited PB was studied with the help of in situ atomic force microscopy (AFM). The in situ AFM images were recorded with lower PB concentrations because the layer thickness achieved in the above-described experiments exceeded the limits of the AFM technique.

Figure 7 shows AFM images recorded in situ during deposition of PB at different deposition potentials with

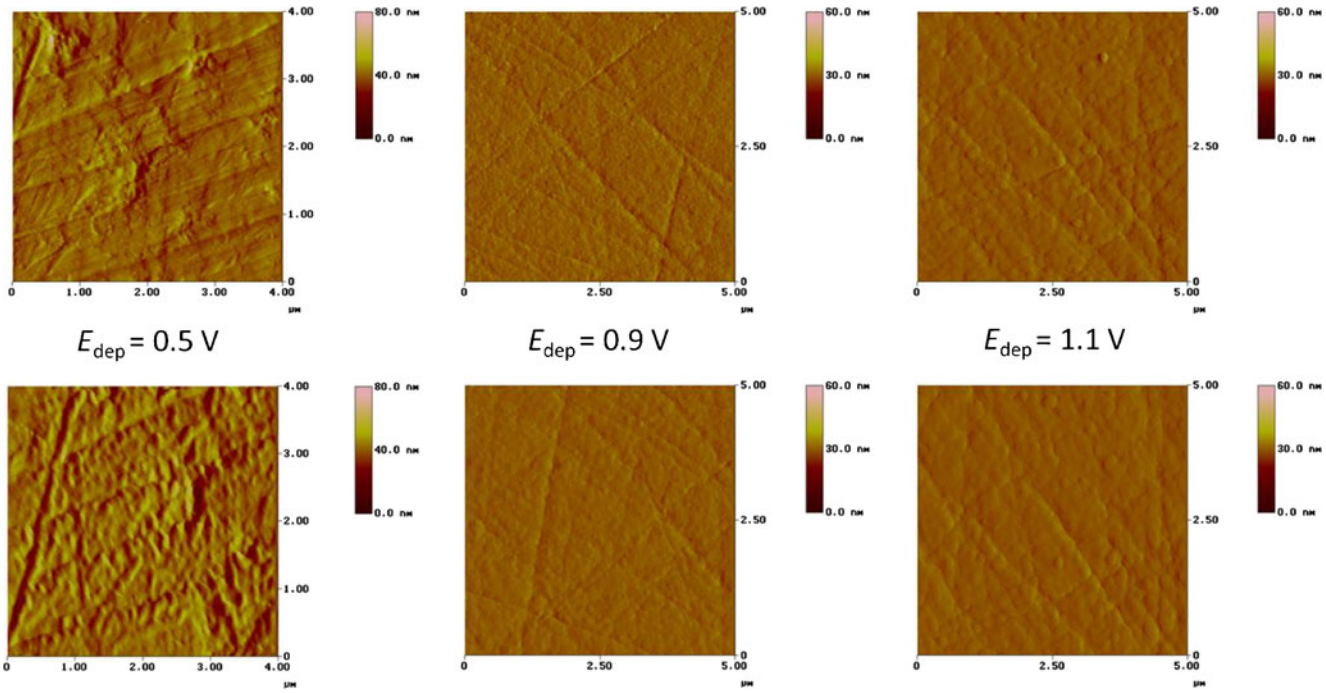

Fig. 7 In situ AFM images of PB film on GC electrode deposited at different E_{dep} before (*upper row*) and after (*lower row*) a deposition time of 220 s

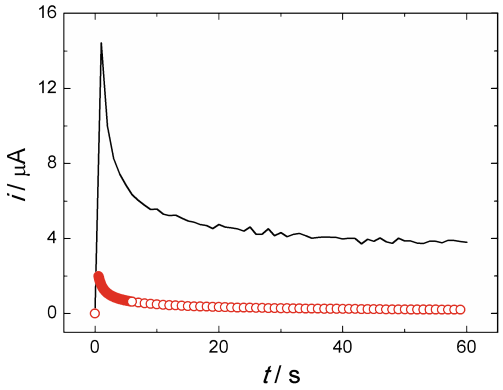

Fig. 9 Simulated current transient (*open circles*) from the Cottrell equation and experimental curve at E=0.8 V

deposition pulses of 220-s length. The results were, in all cases, identical: a dense layer of PB is formed. It was not possible to resolve the PB grains. In this context, and in order to determine the size of the deposited PB particles, similar experiments have been made using a silicon wafer. The PB particles were deposited at E_{dep}=0.45 V during 540 s. Figure 8 shows the AFM image of a silicon sample with deposited PB particles. This image shows that the PB particles have a wide range of sizes: the diameters range from approximately 200 to 550 nm, with an average diameter of about 430 nm. In independent measurement by Laser Doppler Anemometry (Zetasizer Nano-ZS, Malvern Instruments, UK), it was found that the maximum of the particle size distribution was between 420 and 460 nm (on logarithmic size scale a symmetric single distribution peak, i.e., monodisperse distribution, with base limits at 150 and 1,100 nm, and half-height at 250 and 1,000 nm), which is in good agreement with the AFM images.

Discussion

The electrochemical and AFM results show that (a) PB is deposited when the potential of the GC electrode is larger than −0.2 V vs. Hg/Hg_2Cl_2, (b) the PB forms a single layer of particles when the deposit is in the PB state (insulator) and also when it is in the Everitt's salt state, (c) multilayers are deposited at those potentials where the deposit is in the Berlin green state (semiconductor). With that information, we can discuss the current-time traces of PB deposition shown in Fig. 3: In order to simulate the currents of the Cottrell plots (Fig. 3) with the help of the Cottrell equation ($i = n_{(\text{particle})}\text{FA}c_{(\text{particle})}\sqrt{D_{(\text{particle})}/\pi t}$; where $n_{(\text{particle})}$ is the

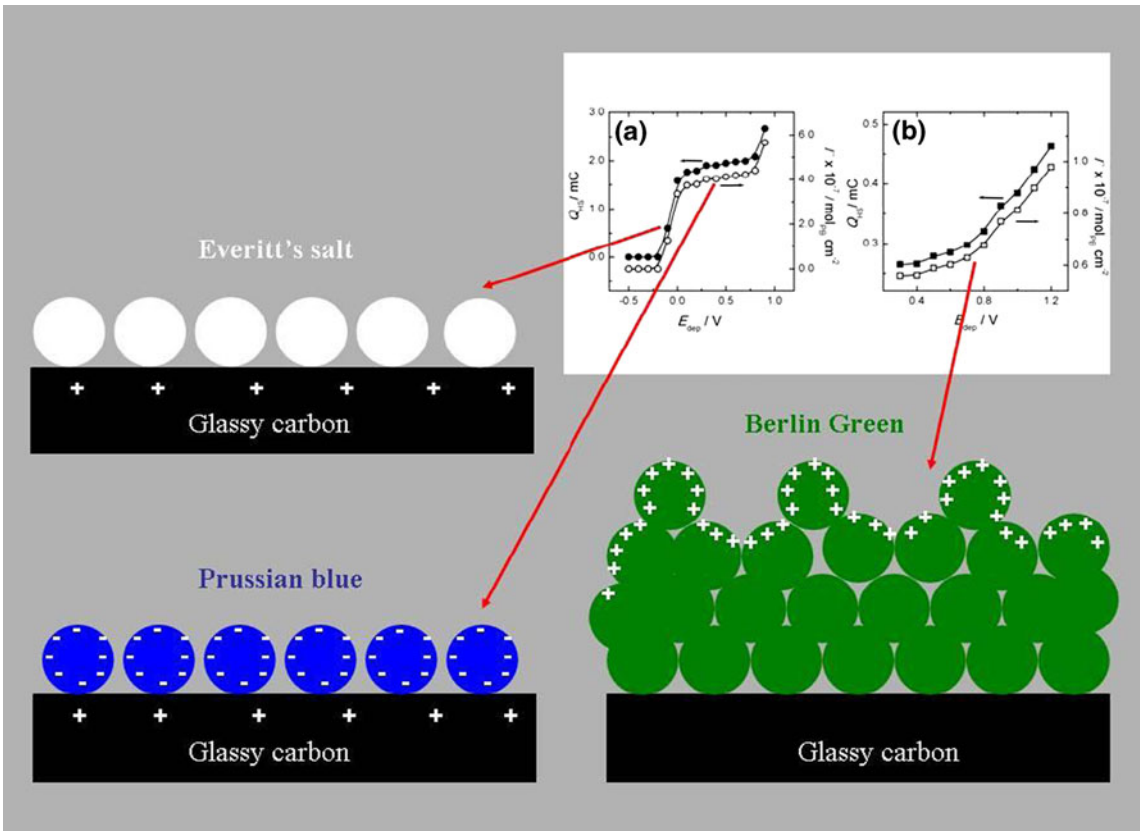

Fig. 10 Schematic presentation of the single layer formation of Prussian blue particles (*left side*) and polylayer formation of Berlin green (*right side*), depending on the deposition potential, and thus on the redox state of the compound on the electrode surface (inset refers to Fig. 5)

number of electrons for the reduction (or oxidation) of one particle!), we have made the following assumptions: (a) at 0.8 V all PB is oxidized to Berlin green (1 electron/2 Fe); (b) PB concentration (determined by ICP analysis of the digested colloidal solution) was 5.4×10^{-3} $mol_{PB}L^{-1}$; (c) average particles diameter $r_{(particle)}$ (from AFM measurements of silicon/PB and from light scattering): 430 nm; (d) diffusion coefficient $D_{(particle)}$ of PB particles (calculated with the help of the Stokes–Einstein equation $D_{(particle)} = k_B T / 6\pi\eta r_{(particle)}$, using average particle radius $r_{(particle)}$ and water viscosity η; k_B is the Boltzmann constant, and T the absolute temperature): 1.14×10^{-8} cm^2 s^{-1}; (e) surface area A of the GC electrode: 0.049 cm^2; (f) with the molar volume of PB (677 cm^3 mol^{-1} [34]), the volume of a colloidal particle (4.16×10^{-14} cm^3), and the Avogadro number, it is possible to calculate the number of electrons $n_{(particle)}$ for the complete oxidation of one PB particle to be 3.76×10^7. In Fig. 9, the simulated i/t transient, in comparison to the experimental curve, is given. Clearly, the simulated currents, which were calculated assuming a complete oxidation of each PB particle, are much smaller than the real currents. This supports our assumption that the overall current is the sum of the faradaic current of PB oxidation (provided that the electrode potential allows this) and the capacitive current due to the reconstruction of the electrode interface.

Conclusions

This work shows that PB can be deposited on a glassy carbon electrode from a colloidal solution provided that the electrode potential is larger than −0.2 V vs. Hg/Hg_2Cl_2. When the PB is neither reduced nor oxidized but remains in the PB state, only a single layer of particles is deposited because the compound is an insulator and cannot assume the electrode potential (Fig. 10). At potentials where Everitt's salt is the thermodynamically stable compound, the deposited PB particles are reduced to Everitt's salt (Fe^{2+}_{hs}) (Fig. 10). Everitt's salt is known to be an insulator, and thus, the single layer cannot grow. Whether the particles of Everitt's salt have a surface charge (like the PB particles) is not known. In case of oxidation of the deposited PB to Berlin green, the particles are semiconducting, and they assume the applied positive electrode potential so that multilayers can be deposited (Fig. 10). The system is interesting because it provides an example of Cottrell behavior, although the measured currents are predominantly of capacitive nature. The reason is that the capacitive currents caused by the reconstruction of the electrode interface are limited by the diffusion of the colloidal particles to the interface. The present paper is a contribution to the understanding of the deposition of redox active colloidal particles on electrodes. It clearly shows that faradaic reactions of the particles during the deposition process can alter the morphology of the deposits. Future activities will be focussed on the deposition of PB on different semiconductor electrodes in order to understand the effect of the base material on deposition.

Acknowledgments We acknowledge the financial support from FONDECYT, Chile, (grant no. 1090217) and from Dirección de Investigación e Innovación of the Pontificia Universidad Católica de Valparaíso (grant no. 037.208/2008 DII-PUCV). E. Muñoz and R. Henríquez additionally thank the Programa Bicentenario de Ciencia y Tecnología, PSD82. R. Cisternas acknowledges kind support of her doctoral scholarship by MECESUP program MECE2/UCH0601 and also by CONICYT.

References

1. Scholz F, Kahlert H (2006) Electrochemistry of polycyanometalates. In: Encyclopedia of Electrochemistry, Edited by A.J. Bard and M. Stratmann; Volume 7b: Inorganic Chemistry. F. Scholz, C. J. Pickett (edts), WILEY-VCH 701–721
2. Araminaitė R, Garjonytė R, Malinauskas A (2010) J Solid State Electrochem 14:149–155
3. Karyakin AA (2001) Electroanalysis 13:813–819
4. Dostal A, Meyer B, Scholz F, Schröder U, Bond AM, Marken F, Shaw SJ (1995) J Phys Chem 99:2096–2103
5. Dostal A, Kauschka G, Reddy SJ, Scholz F (1996) J Electroanal Chem 406:155–163
6. Bárcena-Soto M, Scholz F (2002) J Electroanal Chem 521:183–189
7. Neff VD (1978) J Electrochem Soc 125:886–887
8. Itaya K, Akahoshi H, Toshima S (1982) J Electrochem Soc 129:1498–1500
9. Jia F, Yu C, Gong J, Zhang L (2008) J Solid State Electrochem 12:1567–1571
10. Hermes M, Scholz F (2009) Solid state electrochemical reactions of electroactive micro- and nano-particles in a liquid electrolyte environment. In: Kharton V (ed) Handbook of solid state electrochemistry. Wiley-VCH, Weinheim
11. Scholz F, Dostal A (1995) Angew Chem Int Ed Engl 34:2685–2687
12. Jaiswal A, Colins J, Agricole B, Delhaes P, Ravaine S (2003) J Colloid Interface Sci 261:330–335
13. Lupu S, Totir N (2010) Coll Czech Chem Commun 75:835–851
14. Skoog DA, West DM (1963) Fundamentals of analytical chemistry. Holt, Rinehart and Winston, Inc., USA
15. Paneth F (1914) Phys Z 15:924–929
16. Fajans K, von Beckerath K (1921) 97:478–502
17. Adamczyk Z (2003) Adv Colloid Interface Sci 100/102:267–347
18. Vervey EJW, Overbeek JTG (1948) Theory of the stability of lyophobic colloids. Elsevier, Amsterdam, New York, republished by Dover Publ. Inc., Mineola, 1999
19. Scholz F, Schwudke D, Stößer R, Boháček J (2001) Ecotoxicol environmental safety. Environ Res 49:245–254
20. Lorna N (2006) Surface-supported transition metal hexacyanometallate nanostructured films. Master of Science thesis, Department of Chemistry, National University of Singapore
21. Meyer B, Scholz F, unpublished results
22. Brewer GEF (1983) J Appl Electrochem 13:269–275
23. Orellana M, Ballesteros L, Del Río R, Grez P, Schrebler R, Córdova R (2009) J Solid State Electrochem 13:1303–1308
24. Zamponi S, Kijak AM, Sommer AJ, Marassi R, Kulesza PJ, Cox JA (2002) J Solid State Electrochem 6:528–533

25. Agrisuelas J, Gabrielli C, García-Jareño JJ, Giménez-Romero D, Gregori J, Perrot H, Vicente F (2007) J Electrochem Soc 154: F134–F140
26. Pyrasch M, Toutianoush A, Jin W, Schnepf J, Tieke B (2003) Chem Mater 15:245–254
27. Zhao H, Yuan Y, Adeloju S, Wallace GG (2002) Anal Chim Acta 472:113–121
28. Ellis D, Eckhoff M, Neff VD (1981) J Phys Chem 85:1225–1231
29. Viehbeck A, DeBerry DW (1995) J Electrochem Soc 132:1369–1375
30. Orellana M, Arriola P, Del Río R, Schrebler R, Cordova R, Scholz F, Kahlert H (2005) J Phys Chem B 109:15483–15488
31. Muñoz EC, Henríquez RG, Córdova RA, Schrebler RS, Cisternas R, Ballesteros L, Marotti RE, Dalchiele EA (2011) J Solid State. Electrochem. doi:10.1007/s10008-010-1287-2
32. Xidis A, Neff VD (1991) J Electrochem Soc 138:3637–3642
33. Weber JH, Cheng KH (1979) Anal Chem 796–799
34. Hazen R, Spaulding R, Kasem K (2003) Am J Undergrad Res 2:27–36